revised

Palladium Carbene Complexes for Selective Alkene Di- and Oligomerization

Vsevolod Khlebnikov,[†] Angelo Meduri,[‡] Helge Mueller-Bunz,[†] Tiziano Montini,[‡] Paolo Fornasiero,[‡] Ennio Zangrando,[‡] Barbara Milani*[,‡] and Martin Albrecht*[,†]

[†] School of Chemistry & Chemical Biology, University College Dublin, Belfield, Dublin 4, Ireland

[‡] Dipartimento di Scienze Chimiche e Farmaceutiche, Università di Trieste, Via Licio Giorgieri 1, 34127 Trieste, Italy

* to whom correspondence should be addressed: milaniba@units.it, martin.albrecht@ucd.ie

Abstract. A series of palladium complexes were synthesized that comprise three sterically different *C,N*-bidentate coordinating NHC-pyridine ligands (NHC = N-heterocyclic carbene). In one set, the pyridine and the carbene are linked by a flexible CH_2 group (**a**), in the other two sets, the two ligand units are directly linked and feature a shielding mesityl substituent on the carbene and either an unsubstituted pyridine (**b**) or a xylyl-substituted pyridine unit (**c**). Investigation of the reactivity of cationic complexes $[Pd(C\hat{}N)Me(NCMe)]^+$, **6**, analogues to Brookhart's α-diimine system, towards alkenes showed a strong correlation between the catalytic activity and selectivity and the ligand setting. While **6a** was inactive in ethylene conversion, **6b** afforded low-molecular weight olefins (oligomerization), and **6c** produced exclusively butene (dimerization). With styrene as substrate, exclusive dimerization occurred with all three complexes. Steric and electronic factors were identified that govern the disparate activity and selectivity, and that allow for efficient tailoring of the catalytic performance.

Introduction

While terminal alkene polymerization is a prime success story of organometallic chemistry due to the availability of catalysts with excellent activity and selectivity,[1] the co-polymerization of olefins with polar co-monomers still remains a challenge of paramount interest.[2] Co-polymerization is much desirable for introducing functional groups as it allows surface properties of polyolefins like adhesion, dyeability, or printability to be improved.[2] The search for active catalysts has been substantially impeded by the incompatibility of the active olefin polymerization catalysts, which often comprise an early transition metal, with functional groups in the monomer. As a result, catalyst deactivation in the presence of oxygen- or nitrogen-containing impurities is common. One approach to address this challenge is the use of late transition metals, as they are generally more tolerant to functional groups than early transition metals because of their lower oxidation state and higher electronegativity. Brookhart's seminal work in ethylene homopolymerization catalyzed by α-diimine palladium(II) complexes such as **A** (Fig. 1)[3] initialized substantial further work along these lines[4,5] and, more importantly, provided access to the co-polymerization of terminal alkenes with polar co-monomers.[6] The initially obtained co-polymer had a low content (<12%) of the polar monomer, which was exclusively located in the polymer branches.[6] An improved insertion of the acrylic ester up to 22% was realized when using cyclophane-modified diimine ligands.[7]

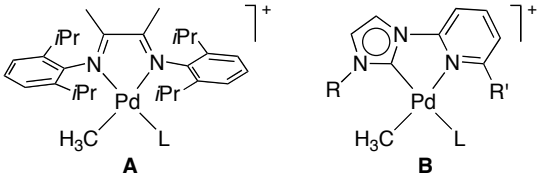

Fig 1. Brookhart's α-diimine palladium catalyst **A** and the carbene-imine palladium surrogate **B**.

A second major breakthrough was reported by Drent with the application of an *in situ* system based on a phosphino-sulfonate ligand and palladium, which induced the formation of ethylene/acrylate co-polymers with the acrylate units incorporated into the main chain.[8] This catalytic system was further exploited by Mecking, achieving up to 52% acrylate insertion into the co-polymer main chain.[9] In addition, the formally neutral *P,O*-bidentate phosphino-sulfonate palladium(II) complexes were active in the co-polymerization of a range of functional substrates, although α-olefin incorporation was relatively poor.[10]

The low productivity of both the *N,N*- and the *P,O*-bidentate catalytic systems has prevented industrial exploitation thus far and has stimulated the search for more efficient catalysts. A

major drawback of Brookhart's complex is the nature of catalyst resting state. Mechanistic studies revealed the formation of a metallacycle due to chelation of the growing polymer chain through coordination of a carbonyl oxygen of an inserted acrylate monomer to the palladium center.[6b] A different resting state has been identified in the catalytic system based on the *P,O* ligands.[9] Metallacycle formation is presumably less favored because of the higher electron density at the *P,O*-chelated metal center. In addition, the reported catalyst systems generally suffer from substantial decomposition of the active species as a consequence of poor thermal stability and a high propensity for irreversible β elimination processes.[6,11]

These issues may be overcome by a desymmetrization of the ligand and by an increase of the Pd–L bond strength. Stronger metal bonding is surmised by using N-heterocyclic carbenes (NHCs), which typically form robust M–C_{NHC} bonds having a substantially higher covalent contribution than traditional donor ligands such as imines or phosphines.[12] Based on these considerations, we aimed at evaluating the catalytic activity of palladium(II) complexes featuring an imine-carbene chelate as in **B** (Fig. 1) as surrogates of Brookhart's catalyst.[13] Here, we report on the synthesis of these complexes with different steric implications and on their reactivity towards substituted and unsubstituted olefins.[14]

Results and discussion

Synthesis and Characterization of the complexes. The pyridyl donor-functionalized imidazolium salts **1a** and **1b** were prepared by established procedures.[15] Imidazolium salt **1c** comprising an *ortho*-xylyl substituent at the pyridine heterocyle was obtained by a related solvent-free quaternization of *N*-mesitylimidazole with 6-xylyl-2-bromopyridine. The imidazolium salts **1** were converted to the corresponding silver carbene complexes **2** by reaction with Ag_2CO_3 in refluxing CH_2Cl_2 in the absence of light (Scheme 1). Successful deprotonation was concluded from the absence of the downfield signal due to the 2*H*-imidazolium proton in the ^{1}H NMR spectra and by comparison of the imidazolylidene ^{1}H NMR signals with related complexes.[16] The structure of complex **2a** was determined earlier to be a halide-bridged dimer, whereas complexes related to **2b** and **2c** were shown to be mononuclear.[16a] Transpalladation with [$PdBr_2$(cod)] (cod = 1,5-cyclooctadiene) afforded the palladium dibromide complexes **3a** and **3b** in high yields and as air-stable solids. Purification of complex **3c** was difficult, perhaps because of steric constraints arising from interference of the bulky xylyl group with the halide ion, leading to partial release of the halide. Pure complexes were only isolated upon conversion of **3c** to the corresponding dicationic bis(acetonitrile) species **4c**. Substitution of the bromide by a smaller MeCN ligand is expected

to relieve the steric strain with the shielding xylyl group. Treatment of complexes **3a** and **3b** with 2 equiv. $AgPF_6$ equally yielded the corresponding dicationic species **4a** and **4b**. All complexes **4** were considerably more soluble in chlorinated solvents and in MeCN than their neutral analogues **3**.

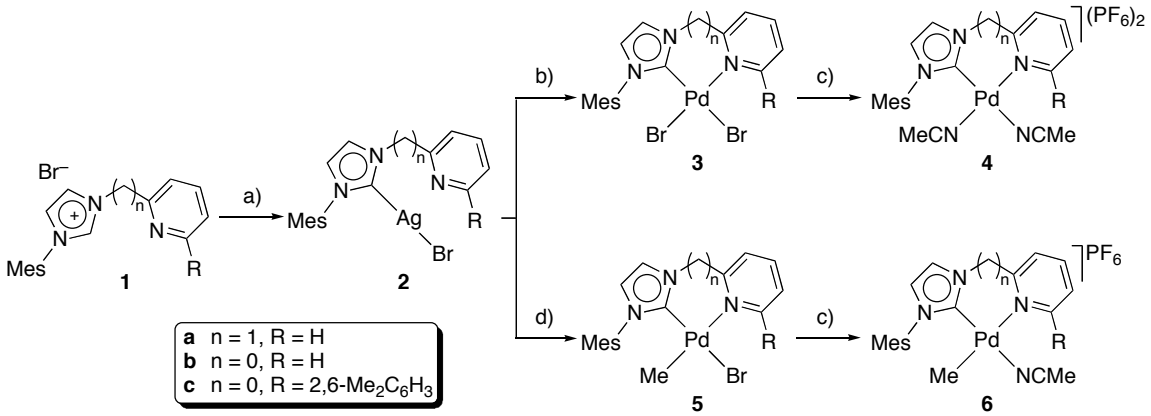

Scheme 1. Synthesis of the complexes (Mes = 2,4,6-$Me_3C_6H_2$); *reactions and conditions:* a) Ag_2CO_3, CH_2Cl_2, reflux; b) [$PdBr_2$(cod)], CH_2Cl_2; c) $AgPF_6$, MeCN; d) [PdMeBr(cod)], CH_2Cl_2 or MeCN.

Due to their limited solubility in chlorinated solvents, complexes **3a** and **3b** were characterized by NMR spectroscopy in DMSO–d_6. Most characteristically, the ^{1}H NMR spectrum of **3a** featured two broad doublets at 5.65 and 5.95 ppm attributed to the CH_2 group interlinking the carbene and pyridine ligand fragments. Variable temperature NMR spectroscopy revealed that these diastereotopic protons exchange slowly at room temperature (Fig. S1).[17] This behavior indicates inversion of the metallacycle on the NMR time scale. Indeed, coalescence of these signals was observed at 45 °C. Similarly, the two *ortho*-methyl groups and the two *meta*-protons of the mesityl substituent appear as two pairs of broad singlets at room temperature that coalesce to single resonances at 40 °C. In contrast, the solvento complex **4a** displays sharp singlets for both the mesityl and the methylene group protons at room temperature in CD_3CN and also in DMSO–d_6 solution, indicative of a fast exchange limit. Inversion of the metallacycle in **4a** is probably accelerated by the facile decoordination of the MeCN ligand as opposed to the more demanding Pd–Br dissociation in **3a**. Ligand dissociation is expected to alter the energy barrier for rotation about the Pd–C_{NHC} and the Pd–N_{py} bonds required for the inversion of the metallacycle. In addition, the smaller size of MeCN as compared to Br facilitates rotation about the N–C_{Mes} bond. The aromatic mesityl proton signals are sharp in complexes **3b** and **3c** and also in **4b** and **4c**. This observation is in agreement with a lower interference of the mesityl wingtip group with *cis*-coordinating ligands as a direct consequence of the unbridged interconnection of the pyridine

and NHC heterocycles. Similarly, the *ortho* methyl groups of the xylyl substituent in **4c** are magnetically equivalent. The metallacycle in these complexes is planar (C_S symmetry) and inversion processes as those in **3a** or **4a** cannot occur. This planar arrangement confines the α-positioned pyridine proton in close proximity to the bromide ligand in **3b**, resulting in a pronounced downfield shift of its proton resonance (δ_H 9.31 compared to 8.63 in **4b**). This interaction is less pronounced in the non-planar system **3a** (δ_H 9.03 *vs* 8.71 in **4a**).

Single crystals suitable for an X-ray diffraction analysis were grown for complexes **3b** and **4a**. The molecular structures (Fig. 2) confirm the structure surmised from solution analyses. In particular, the planes of the heterocyclic rings in **3b** coincide with the planar metallacycle, whereas in **4a**, these planes are twisted out of the distorted metal square plane (torsion angles 35–40°). The different Pd–Br distances in **3b** reflect the substantial electronic asymmetry of the NHC-pyridine ligand (2.4179(3) for Pd–Br1 *trans* to pyridine and 2.4714(3) Å for Pd–Br2 *trans* to NHC). This effect is even more pronounced in the dicationic complex **4a**, where the Pd–NCMe bond lengths differ by almost 0.1 Å (2.077(1) Å *vs* 1.987(1) Å). Moreover, the direct linkage of the two heterocycles in **3b** induces a substantial yaw distortion[18] (θ 14.4° in **3b** compared to 6.3° in **4a**). This distortion forces the mesityl wingtip group to be oriented away from the *cis*-positioned substituent, while in **4a**, this substituent points towards this position, commensurate with the hindered rotation about the N–C_{Mes} bond observed in the NMR spectroscopic analyses of the methylene-bridged complex **3a**.

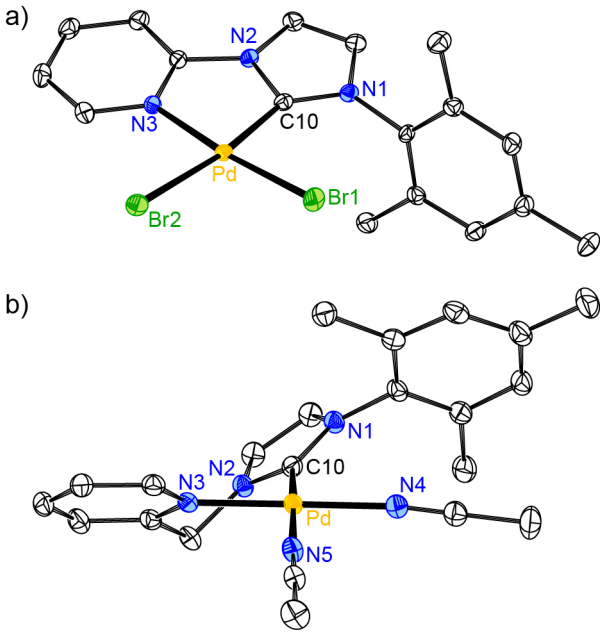

Fig. 2 ORTEP plot of complexes **3b** and **4a** (50% probability, hydrogen atoms, co-crystallized solvent molecules and PF_6^- counterions of **4a** omitted for clarity). Selected bond lengths (Å) and angles (deg) for **3b**: Pd–C10 1.965(2), Pd–N3 2.0578(17), Pd–Br1 2.4179(3), Pd–Br2 2.4714(3); C10–Pd–N3 79.78(8), N1–C10–Pd

142.04(16), N2–C10–Pd 113.34(14). For **4a**: Pd–C10 1.9592(15), Pd–N3 2.0215(13), Pd–N4 2.0774(14), Pd–N5 1.9866(14); C10–Pd–N3 87.83(6), N1–C10–Pd 133.39(12), N2–C10–Pd 120.80(11).

The understanding gained from complexes **3** and **4** was subsequently used to generate monocationic methyl palladium complexes comprising an imine-carbene ligand. Thus, transpalladation of the silver carbene complexes **2** with [PdMeBr(cod)] afforded the expected neutral complexes **5a** and **5b** as off-white air-stable solids. Spectroscopic data for **5a** were in agreement with literature data.[16b] A single set of resonances was observed for **5b**, indicative of the formation of a single isomer.[14a] The signal at 0.00 ppm in the ^{1}H NMR spectrum and at –14.0 ppm in the ^{13}C NMR spectrum was assigned to the palladium-bound methyl group, while a weak resonance at δ_C 170.2 ppm was attributed to the carbene nucleus. The single resonances of the aromatic mesityl protons (δ_H 7.06) and the *ortho* Me groups (δ_H 2.05) indicate fast rotation about the N–C_{Mes} bond. Moreover, the pronounced low-field shift of the pyridine α proton supports an interaction of this nucleus with bromide (see above), thus suggesting a configuration as suggested in Scheme 1 with the Me group and the carbene in a mutual *cis* arrangement. A nuclear Overhauser effect (NOE) between the palladium-bound methyl group and the *ortho* methyl groups of the carbene-bound mesityl unit confirmed this assignment.

Further structural information was obtained by a single crystal X-ray diffraction analysis of **5b**. The molecular structure (Fig. 3) is similar to that of **3b** (vide supra) and features the methyl group *trans* to the pyridine ligand as inferred from solution. The observed configuration corresponds to the thermodynamically expected product when considering the relative *trans* influence of the ligands, NHC > pyridine and Me > Br. Bond lengths and angles around the metal center including the yaw distortion are highly similar to those in **3b** except for the Pd–N3 bond, which is here substantially longer (2.158(2) *vs* 2.022(1) Å in **3b**). The increase is a direct consequence of the strong *trans* influence of the methyl group and suggests some flexibility of the bidentate chelate.

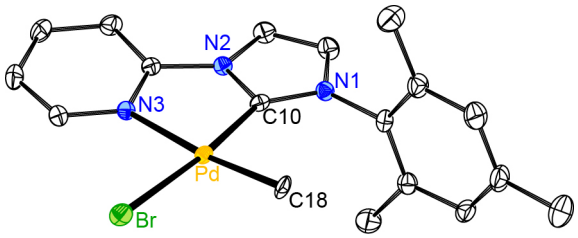

Fig. 3 ORTEP plot of complex **5b** (50% probability, hydrogen atoms and co-crystallized CH_2Cl_2 molecule omitted for clarity). Selected bond lengths (Å) and angles (deg): Pd–C10 1.972(2), Pd–C18 2.062(2), Pd–N3 2.1575(18), Pd–Br 2.4811(3), C10–Pd–N3 79.06(8), N1–C10–Pd 142.29(16), N2–C10–Pd 114.19(15).

In line with the difficulties encountered in the isolation of **3c**, complex **5c** could not be purified satisfactorily and was instead subjected to halide abstraction. Treatment of complexes **5** with $AgPF_6$ readily yielded the monocationic complexes **6**. The NMR spectra of all complexes showed a single set of resonances, which is in agreement with the formation of one isomer exclusively. The ^{1}H NMR spectra in CD_3CN featured for all complexes a resonance around 0.00 ppm, which was attributed to the Pd–Me unit. NOEs were observed between this methyl group and the *ortho* methyl groups of the mesityl ligand, but not with the *ortho* proton or the substituent at pyridine. Accordingly, the deduced structure in solution features the methyl group *cis* to the NHC unit (and *trans* to the pyridine), as expected when considering the relative *trans* influence of the ligands. In ^{13}C NMR spectroscopy this group resonates at –13.0, –10.9, and –8.5 ppm for complexes **6a–c**, respectively. The carbene carbon signal shifted to slightly higher field with respect to the neutral complexes **5** and was observed around 168.0 ppm for all three complexes. Sharp singlets for the protons of the mesityl and xylyl substituents indicate fast rotation of these groups on the NMR time scale. As observed for the dicationic MeCN complex **4a**, metallacycle inversion in **6a** is rapid and the methylene group appears as a singlet at δ_H 5.48.

Steric aspects were further investigated by single crystal analyses of complexes **6**. The molecular structures of the cationic complexes (Fig. 4) comprise the palladium center in a distorted square-planar geometry. As expected from thermodynamic considerations (*trans* influence of the ligands), the coordinated solvent molecule is *trans* to the carbene ligand, and the methyl group and the pyridine are mutually *trans*. The presence of a single isomer suggests the same configuration to be preserved in solution (*cf* NOE experiments). The methylene bridge in **6a** induces a wider ligand bite-angle than in **6b** and **6c**, and forces the ligand into a puckered conformation, reflected by a dihedral angle of ca. 40° between each heterocycle and the metal coordination plane. Despite these differences, the Pd–C_{NHC}, the Pd–C_{Me}, and also the Pd–N_{MeCN} bond lengths display little variation in the three complexes. However, the Pd–$N_{pyridine}$ bond is distinctly longer in complex **6c** (Pd1–N3 2.2129(13) Å) than in complexes **6a** or **6b** (2.1616(15) Å and 2.1391(11) Å, respectively). This difference is most probably a direct consequence of the intramolecular steric repulsion induced by the bulky xylyl substituent of the pyridine ring in **6c**. Similarly the $N_{pyridine}$–Pd–N_{MeCN} angle increases from **6a** < **6b** < **6c** (94.06(6)°, 94.96(5)°, and 103.59(5)°, respectively), which lends further support to such a hypothesis. In addition, the NCMe ligand in **6c** is substantially bent

out of the metal coordination axis (Pd–N4–C19 167.31(12)°), while in **6b**, an almost linear ligand arrangement was established (Pd–N4–C19 176.66(12)°). These interferences are expected to be even more pronounced when a bulky bromide is coordinated *cis* to the xylyl-substituted pyridine ligand, which corroborates the difficulties encountered in the isolation and purification of the neutral complexes **3c** and **5c** (see above).

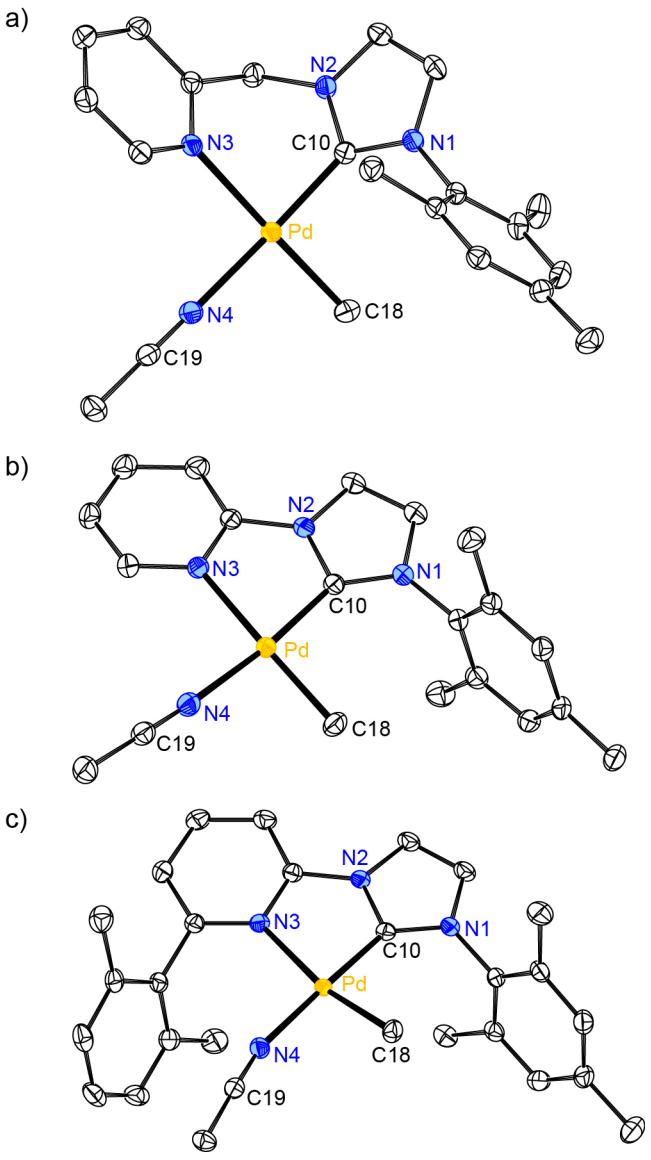

Fig 4. ORTEP representation of the molecular structure of **6a** (a), **6b** (b), and **6c** (c); all thermal ellipsoids at 50% probability level, hydrogen atoms omitted for clarity.

Table 1. Selected bond lengths (Å) and angles (deg) for complexes **6**

	6a	**6b**	**6c**
Pd–C10	1.9605(18)	1.9757(13)	1.9624(14)
Pd–C18	2.0350(19)	2.0375(14)	2.0395(15)
Pd–N3	2.1616(15)	2.1391(11)	2.2129(12)

Pd–N4	2.0650(16)	2.0511(12)	2.0571(12)
C10–Pd–N3	86.39(7)	79.37(5)	77.93(5)
C10–Pd–N4	176.38(7)	174.03(5)	178.42(5)
N3–Pd–N4	91.06(6)	94.96(5)	103.59(5)
Pd–N4–C19	170.08(16)	176.66(12)	167.31(12)
N2–C10–Pd–N3	36.50(14)	1.59(9)	10.09(10)

Reactivity and Catalysis. The insertion of ethylene into the metal-alkyl bond represents a key step in the single-site metal-catalyzed homo- and co-polymerization of alkenes. Thus, the reactivity of complexes **6** with ethylene was investigated by in situ NMR experiments performed by saturating a 10 mM CD_2Cl_2 solution of each complex with ethylene at room temperature. Spectroscopic analyses revealed markedly different reactivity pattern for the three complexes. Complex **6a** comprising a flexible chelate with the heterocycles bent out of metal coordination plane was catalytically silent and no substrate conversion was detected after 15 h.[19] In contrast, complexes **6b** and **6c** with rigidly planar ligands showed catalytic activity. When a solution of complex **6b** was treated with ethylene, the ^{1}H NMR spectrum recorded 25 min after introducing the alkene showed the presences of **6b** together with additional resonances at 1.58 and 5.45 ppm that are indicative of the formation of *cis*- and *trans*-2-butene. Furthermore, signals at 6.0 (multiplet), 5.0 (two doublets) and below 2.0 ppm suggest the formation of terminal olefins including 1-butene and higher α-olefins (Fig. S2).[17,20] Such products are obviously the result of ethylene insertion into the Pd–H bond and subsequent (multiple) insertion of ethylene into the Pd–ethyl fragment, followed by β hydrogen elimination. Further monitoring of the reaction for 5 h revealed a gradual increase in the concentrations of butenes and higher olefins and a slight decrease of the concentration of **6b** (ca. 5% over 4 h, Fig. 5a), which is accompanied by a slow increase in resonances attributed to a Pd–ethyl species and to propene. Propene resulted from direct ethylene insertion into the Pd–Me bond, followed by β hydrogen elimination with the concomitant formation of the Pd-H intermediate.[21] The formation of these products (ca. 5% over 4 h) correlates well with the decrease of **6b** and points to a slow activation of **6b**, *i.e.* only a small fraction of the catalyst precursor is effectively active in olefin di- and oligomerization.

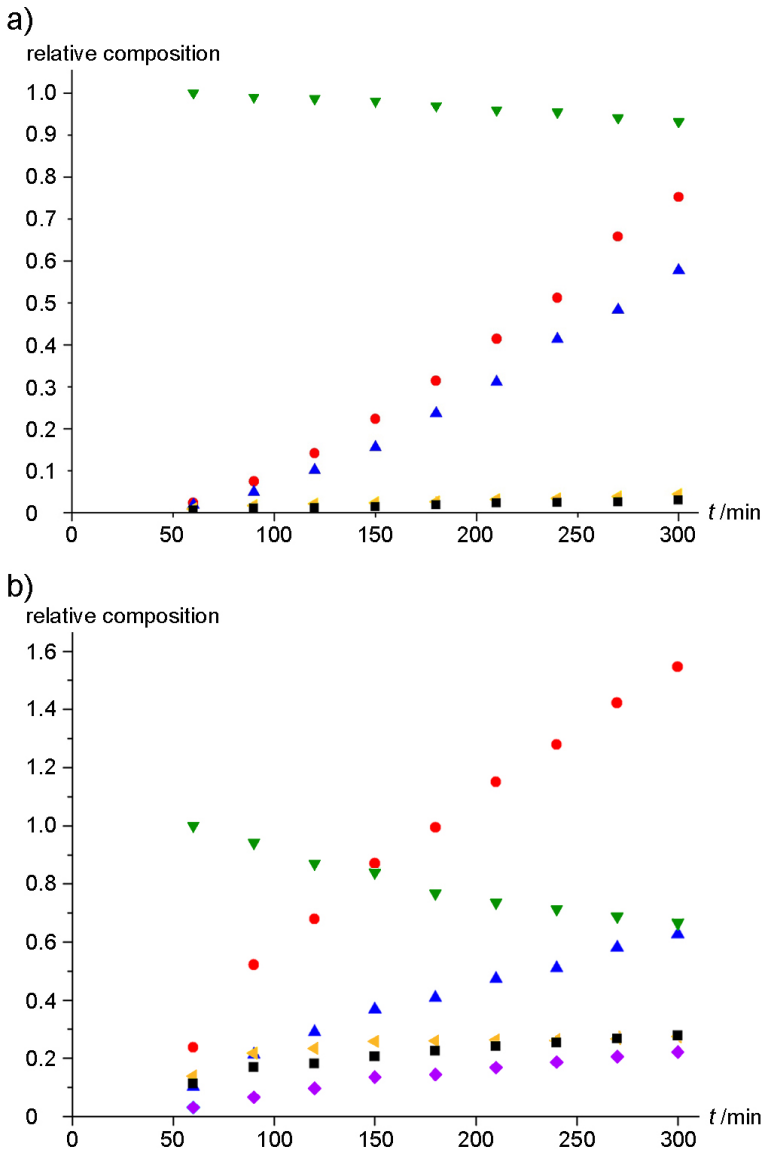

Fig 5. Time-dependent composition of the reaction of complex **6b** (a) and **6c** (b) with ethylene in NMR tube experiments (integrals normalized to the Pd–CH_3 group after 1 h incubation, $C_2H_2Cl_4$ as internal standard). Key to symbols: ▼ complex **6**, ● 2-butenes, ▲ 1-butene and (for Fig. 5a only) higher olefins, ◄ Pd–ethyl species, ■ propene, ◆ imidazolium salt.

In an identical experiment, complex **6c** comprising aryl substituents on both sides of the *C,N*-bidentate chelate afforded butene isomers as the major product along with propene (Fig. S3).[17] Unlike the reactions with **6b**, no formation of higher α-olefins was detected. Time-resolved ^{1}H NMR spectroscopic monitoring of the reaction of **6c** with ethylene showed that the Pd–Me resonance of original palladium complex is reduced to about 65% within the first 5 h of reaction (Fig. 5b). During this time, resonances due to propene and a Pd–ethyl species grew by some 10–15%. In addition, the appearance of signals attributed to an imidazolium salt akin to **1c** was identified by the diagnostic low-field resonance of the C2-bound imidazolium proton at δ_H 9.31 ppm. This signal increased to about 20%, suggesting partial

cleavage of the Pd–C_{NHC} bond. The sum of imidazolium and Pd–ethyl species corresponds well with the amount of **6c** that is consumed over the measured time span. From integration of the terminal CH_3 groups for propene, 1-butene, and *cis*- and *trans*-2-butene, a rate for ethylene consumption has been deduced under the assumption that the quantity of generated propene is identical to the quantity of activate palladium complex. Accordingly, the rate of the reaction is ca. 7.1 h^{-1} (mol ethylene per mol catalyst in the first hour) under these NMR specific conditions (high Pd concentration, 1 bar ethylene). The calculated rate gradually decreases to 3.3 h^{-1} after 5 h, because decomposition of the active species to the imidazolium salt becomes competitive and thus makes an estimation of the active species highly uncertain.[22]

Comparison of the reaction profiles of **6b** and **6c** discloses a number of distinct differences. Firstly, activation of complex **6c** is significantly faster than that of **6b**, 35% *vs* 5% during a 5 h reaction time. Faster activation might be related to a faster exchange of the bonded MeCN with ethylene as a direct consequence of the longer Pd–N4 distance in **6c** than in **6b** (Table 1). Faster activation is also reflected by the higher yield of products.[23]

Secondly, the catalyst derived from **6c** induces exclusive formation of butenes. This product selectivity is generally assumed to originate from double ethylene insertion into a metal hydride species, involving a Cossee-type mechanism.[24] Most presumably, the steric shielding in **6c** imparted by the bulky mesityl and xylyl substituents effectively reduces the stability of the putative C_4-palladium intermediate. This destabilization promotes elimination reactions and effectively inhibits the formation of higher olefins, thus providing a methodology for the selective alkene dimerization that may not involve a metallacyclic intermediate as in related chromium-catalyzed reactions.[25] In **6b**, the shielding of the palladium coordination sphere is much less effective (*cf* the different stability of the bromide complexes **4b** and **4c**), and further ethylene insertion may thus ensue. However, the less shielded site is *trans* to the Pd-carbene bond and this configuration may promote β hydrogen elimination and hence only a small number of ethylene insertion cycles may be accomplished. Such a model rationalizes the formation of low-molecular weight alkenes like hexene, octene, and decene. The observed differences between **6b** and **6c** strongly suggests a ligand-induced selectivity of product formation, which implies that the catalytically active species contains the ligand and does not form after ligand dissociation.

Furthermore, polymerization is probably prevented by the reduced space around palladium in complexes **6** compared to Brookhart's catalyst. The close proximity of the palladium center and the aryl groups in **6** likely destabilizes the bonding of long alkyl chains and therefore

leads to oligomers only. In Brookhart-type catalysts such as in [PdCl(Me)(Me-BIAN)], **7** (Me-BIAN = bis(2,6-Me_2-phenyl)-acenapthenequinonediimine, (2,6-$(CH_3)_2$-$C_6H_3)_2$-BIAN; Fig. 6), the distance between the palladium-bound nuclei and the closest aryl ring is 3.95 and 4.32 Å for the Me···centroid and Cl···centroid, respectively. In the structures of complexes **6**, the corresponding Me···centroid distances are substantially shorter, 3.81 Å and 3.53 Å for C18···centroid in **6b** and **6c**, respectively, and a mere 3.17 Å for N4···centroid in **6c**. This congestion supports an enhanced steric shielding of the palladium center and of the *cis*-bound ligands in complexes **6b** and **6c** compared to **7**.

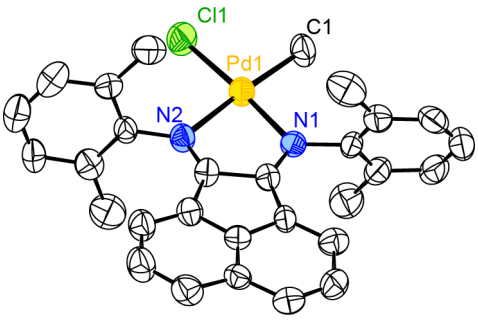

Fig 6. ORTEP representation of one of the two independent complexes of **7** (thermal ellipsoids at 50% probability level, hydrogen atoms omitted for clarity). Selected bond lengths (Å) and angles (deg): Pd1–N1 2.088(6), Pd1–N2 2.203(5), Pd1–C1 2.039(6), Pd1–Cl1 2.283(2), N1–Pd1–N2 79.8(2). The other complex has a disordered Me/Cl ligand (see experimental section).

And thirdly, the catalytically active species derived from **6c** is considerably less stable than that generated from **6b**, and substantial quantities of imidazolium elimination occurred. Even though a Pd–ethyl species appears to be the catalyst resting state for both catalytic systems, reductive elimination takes place from the palladium hydride species only (*cf* formation of 2-*H*-imidazolium salt).[26] Hence, reductive elimination is in competition with insertion of ethylene to reach the catalyst resting state. The propensity of the (hydride)(carbene)palladium intermediate to undergo imidazolium elimination[27] corroborates the notorious difficulties in using NHCs as ligands in polymerization catalysts.[28]

In an attempt to stabilize the putative Pd–ethyl intermediate for isolation, the MeCN ligand in complexes **6b** and **6c** was substituted by γ-picoline.[29] However, catalytic experiments with these modified complexes did not afford any detectable quantities of the insertion products and no resonances were observed that could be tentatively attributed to a Pd–ethyl species.[21]

Larger scale reactions were performed in a 25 mL Büchi "tinyclave steel" reactor using ethylene (2.5 bar). Dibromomethane (CH_2Br_2) was the solvent of choice as its solvating properties are similar to CD_2Cl_2 used in the NMR studies, yet its higher molecular weight does not interfere with the signals of alkenes in GC-MS analyses. Reactions catalyzed by

complex **6b** at 35 °C afforded a mixture of butenes and low molecular-weight alkenes. The relative product distribution deduced from GC-MS measurements after 24 h was C_4H_8 (0.85), C_6H_{12} (1.0), C_8H_{16} (0.37), and $C_{10}H_{20}$ and higher (0.07; Fig. S4).[17]

Such mixtures of C_4–C_{10} linear alkenes are of growing interest for use as co-monomers with ethylene to yield branched linear low-density polyethylene (LLDPE) and for the synthesis of lubricants.[30] In contrast, reactions carried out with complex **6c** as catalyst precursor only afforded propene and isomers of butenes. These results are in good agreement with the NMR spectroscopic studies. During the reaction in the autoclave, both complexes **6b** and **6c** completely decomposed to palladium black and the corresponding imidazolium salt.

Expansion of the substrate scope to styrene as a terminal olefin did not reveal any conversion in CH_2Br_2, at 35 °C or 50 °C, but solely complex degradation was observed even in the presence of excess 1,4-benzoquinone (BQ; [BQ]/[**6**] = 40).[31] Changing the solvent to protic and polar 2,2,2-trifluoroethanol (TFE) had a beneficial effect on catalyst activity and stability.[32] In reactions performed at 50 °C in the presence of a large excess of substrate ([styrene]/[**6**] = 6800; Table 2, entries 1–3), styrene was converted with all three complexes **6a–c** highly chemo- and stereospecifically to the head-to-tail dimer *E*-1,3-diphenyl-1-butene as the exclusive product.[33] No products resulting from oligo- or polymerization were detected. In addition, the reaction remained visually homogeneous and no complex degradation was observed. The stabilizing effect imparted by TFE has previously been attributed to an extended lifetime of the palladium hydride intermediate, which allows for styrene insertion and the induction of a new catalytic cycle.[32] In contrast to reactions with ethylene, complex **6a** featuring a flexible methylene linker in the chelating ligand was catalytically active and achieved appreciable 230 turnovers in 24 h. Complex **6b** displayed very low activity and afforded only a small quantity of dimeric product, turnover number (TON) was 32. The most sterically demanding complex **6c** showed highest performance and a TON = 500 was achieved. The catalytic activity slightly diminished upon increasing the reaction temperature (entries 4, 5), which may be a consequence of the limited stability of the intermediate palladium hydride species (*vide supra*). No di- or oligomeric products were obtained from reactions performed in EtOH at 60 °C, pointing to a delicate role of the solvent in the activation of the catalyst precursor. Whereas for both ethylene oligomerization and styrene dimerization the active species is a Pd–H intermediate, it is worth noting that with styrene, no products were observed that originate from alkene insertion into the Pd–Me bond. This result and the strong solvent dependence suggest a different catalyst activation pathway for ethylene and styrene conversion. While in the former, evidence for the formation of propene points to

olefin insertion into the Pd–Me bond, for styrene, TFE seems to be involved in the activation step leading to the formation of the catalytically competent Pd–H species. A possible pathway is depicted in Scheme 2 and comprises the protonolysis of the Pd–Me bond with concomitant formation of methane and a Pd-trifluoroalkoxide, followed by β hydrogen abstraction and the elimination of trifluoroacetaldehyde.[34]

Table 2. Catalytic dimerization of styrene [a]

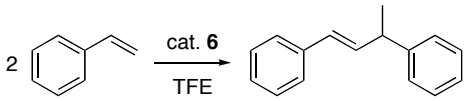

Entry	cat.	T (°C)	TON[b]
1	**6a**	50	230
2	**6b**	50	32
3	**6c**	50	500
4	**6c**	60	500
5	**6c**	70	440

[a] Reaction conditions: [**6**]/[BQ]/[styrene] 1:40:6800 in TFE (20 mL, 0.64 mM in **6**). [b] TON as mol product/mol catalyst after 24 h determined by GC and averaged over at least 2 runs.

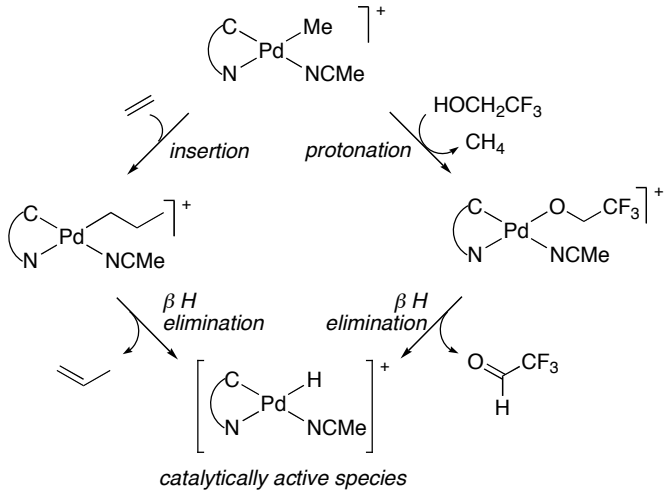

Scheme 2. Suggested pathways for the activation of the catalyst precursor with ethylene/CH_2Cl_2, and with styrene/trifluoroethanol (TFE).

Experiments aimed at co-polymerizing ethylene and styrene were performed with complex **6c** in TFE at 50 °C and under moderate ethylene pressure (1.5 bar). Under comparable conditions ([styrene]/[BQ]/[**6c**] = 6800:40:1), stereoselective formation of the dimer *E*-1,3-diphenyl-1-butene occurred (TON = 61), but no ethylene conversion was detected. The

activity was considerably lower than in the absence of ethylene (TON = 500, *cf* Table 2 entry 3).

Addition of CH_2Br_2, *i.e.* the solvent used for ethylene di- and oligomerization, did not alter the course of the reaction but decreased the styrene dimerization rate. At a 9:1 ratio of TFE/CH_2Br_2, 33 turnovers were recorded after 24 h, while further enhancement of the CH_2Br_2 fraction (1:9 ratio TFE/CH_2Br_2) completely suppressed styrene dimerization. No ethylene was consumed in any of these experiments. These results support a different mode of activation of the palladium complexes **6** for styrene and for ethylene dimerization. Likewise, ethylene/methyl acrylate copolymerization in THF or in toluene (1.5 bar, 35 °C) gave no polymerization products and instead induced complex decomposition irrespective of the ligand arrangement in the catalyst precursor complexes **6**.

Conclusions

New pyridine-functionalized NHC palladium complexes were synthesized as catalyst precursors for the conversion of olefins. Modification of the steric impact of the *C,N*-bidentate ligand was used to tailor the activity and selectivity of the palladium center. A clear relationship between the ligand structure and the activity and selectivity of the catalytic reaction was demonstrated. Precatalyst **6a** featuring a pyridine and a carbene binding site linked by a methlyene group was inactive, while **6b** and **6c** comprising the two heterocycles directly connected were both active, yet displayed different product selectivity. Selective dimerization of ethylene was observed with sterically demanding ligands (as in **6c**), while omission of the shielding xylyl group on the pyridine ring (as in **6b**) results predominantly in oligomerization reactions. The use of styrene as a higher olefin revealed that dimerization is regiospecific. The selectivity towards dimerization may be rationalized by the impact of the two shielding groups on the pyridyl-NHC ligand in **6c**, which interact with *cis*-coordinated ligands. This shielding prevents the coordination of bulky groups such as a growing polymer chain, and facilitates β hydrogen elimination. The limited stability presumably originates from the facile reductive elimination from transient Pd–H species, which results in imidazolium salt formation. Such decomposition pathways are in line with the previously reported poor performance of other NHC complexes in polymerization reactions. These results may provide further guidance for the design of efficient polymerization and oligomerization catalysts based on functional group-tolerant late transition metals.

Experimental

General. The preparation of 2-bromo-6-(2,6-dimethylphenyl)pyridine,[35] *N*-mesityl-*N*′-(2-pyridylmethyl)imidazolium bromide **1a**, *N*-mesityl-*N'*-2-pyridylimidazolium bromide **1b**,[15a] the silver complex **2a**,[16a] complex **5a**,[16b] complex **7**,[36] and the metal precursors [PdBr(Me)(cod)], [PdCl(Me)(cod)], and [$PdBr_2$(cod)][37] were published elsewhere. All other reagents were purchased from commercial sources and used without further purification. ^{1}H and $^{13}C\{^1H\}$ NMR spectra were recorded at room temperature on Varian spectrometers operating at 400 or 500 MHz unless stated otherwise. Chemical shifts (δ in ppm, *J* in Hz) were referenced to $SiMe_4$. Signal assignments are based on homo- and heteronuclear (multiple-bond) correlation spectroscopy. Microanalyses were performed with an Exeter Analytical instrument CE-440. HRGC analyses were run on a Carlo Erba HRGC 5300 Mega Series equipped with a SE 30 capillary column (30 m × 0.32 mm), carrier gas He (50 KPa), split 1:60. GC/MS analyses were performed with an Agilent GC 7890 instrument using a DB-225ms column (J&W, 60m, 0.25mm ID, 0.25micron film) and He as carrier coupled with a 5975 MSD. High resolution mass spectrometry was carried out with a Micromass/Waters Corp. USA liquid chromatography time-of-flight spectrometer equipped with an electrospray source.

Compound 1c. A mixture of 2-bromo-6-(2,6-dimethylphenyl)pyridine (0.23 g, 1.2 mmol) and 1-mesitylimidazole (0.32 g, 1.2 mmol) was kept neat at 175°C for 24 h. After cooling, the solid formed was washed with Et_2O and dried in *vacuum*. Yield: 0.39 g (72%). MS (ES): *m/z* 369, $[M]^+$. ^{1}H NMR ($CDCl_3$, 400 MHz, 298K): δ 11.36 (s, 1H, NCHN), 9.14 (d, $^3J_{HH}$ = 7.9 Hz, 1H, H^3_{py}), 8.86 (t, $^3J_{HH}$ = 1.6 Hz, $^4J_{HH}$ = 1.6 Hz, 1H, H_{imi}), 8.14 (t, $^3J_{HH}$ = 7.9 Hz, $^3J_{HH}$ = 7.9 Hz, 1H, H^4_{py}), 7.38 (d, $^3J_{HH}$ = 7.9 Hz, 1H, H^5_{py}), 7.33 (t, $^3J_{HH}$ = 1.6 Hz, $^4J_{HH}$ = 1.6 Hz, 1H, H_{imi}), 7.22 (t, $^3J_{HH}$ = 7.6 Hz, $^3J_{HH}$ = 7.6 Hz, 1H, H^4_{Ar}), 7.11 (d, $^3J_{HH}$ = 7.6 Hz, 1H, H^3_{Ar}+ H^5_{Ar}), 7.00 (s, 2H, H_{Mes}), 2.31 (s, 3H, *p*-mesityl Me), 2.16 (s, 6H, *o*-mesityl Me), 2.05 (s, 6H, *o*-Ar Me). $^{13}C\{^1H\}$ NMR ($CDCl_3$, 100 MHz, 298K): δ 159.9 (C_{py}), 146.0 (C_{py}), 141.9 (C_{Mes}), 141.6 (C^4_{py}), 138.9 (C_{Ar}), 136.5 (NCN), 136.1, 134.3, 130.9, 130.4, 129.0, 128.2 (6 × C_{Ar+Mes}), 126.9 (C^5_{py}), 124.3 (C_{im}), 120.5 (C_{im}), 114.7 (C^3_{py}), 21.5 (*p*-mesityl Me), 20.7 (*o*-Ar Me), 17.8 (*o*-mesityl Me). Anal. Calcd. for $C_{25}H_{26}BrN_3$ (448.40): C 66.96, H 5.84, N 9.37. Found: C 66.56, H 5.63, N 9.27.

Complex 2b. *N*-Mesityl-*N*′-2-pyridylimidazolium bromide **1b** (1.00 g, 2.90 mmol) was refluxed with Ag_2CO_3 (0.48 g, 1.7 mmol) in CH_2Cl_2 (50 ml) for 18 h. The reaction mixture

was then filtered through celite and volatiles were removed under reduced pressure. The resulting brown solid was washed with Et_2O and dried *in vacuum*. Yield 1.21 g (92%). Recrystallization from CH_2Cl_2/Et_2O gave an analytically pure sample. MS (ES): *m/z* 633, $[Ag(ligand)_2]^+$. ^1H NMR ($CDCl_3$, 400 MHz, 298K): δ 8.50 (dd, $^3J_{HH}$ = 4.8 Hz, $^4J_{HH}$ = 1.5 Hz, 1H, H^6_{py}), 8.24 (d, $^3J_{HH}$ = 7.8 Hz, 1H, H^3_{py}), 8.09 (d, $^3J_{HH}$ = 1.9 Hz, 1H, H_{imi}), 7.88 (td, $^3J_{HH}$ = 7.8 Hz, $^4J_{HH}$ = 1.5 Hz, 1H, H^4_{py}), 7.37 (ddd, $^3J_{HH}$ = 7.8 Hz, $^3J_{HH}$ = 4.8 Hz, $^4J_{HH}$ = 0.8 Hz, 1H, H^5_{py}), 7.07 (d, $^3J_{HH}$ = 1.9 Hz, 1H, H_{imi}), 6.94 (s, 2H, H_{Mes}), 2.31 (s, 3H, *p*-mesityl Me), 2.00 (s, 6H, *o*-mesityl Me). $^{13}C\{^1H\}$ NMR ($CDCl_3$, 100 MHz, 298K): δ 150.6 (C^2_{py}), 148.9 (C^6_{py}), 139.7 (C_{Mes}), 139.5 (C^4_{py}), 135.6, 134.5, 129.5 (3 × C_{Mes}), 123.9 (C^5_{py}), 123.1 (C_{Im}), 120.1 (C_{Im}), 115.5 (C^3_{py}), 21.1 (*p*-mesityl Me), 17.8 (*o*-mesityl Me). The carbene carbon was not observed. Anal. Calcd. for $C_{17}H_{17}AgBrN_3$ (451.11) × 1/4 CH_2Cl_2: C 43.86, H 3.73, N 8.90. Found: C 44.25, H 3.85, N 8.92.

Complex 2c. Compound **1c** (0.67 g, 1.5 mmol) was refluxed with Ag_2CO_3 (0.46 g, 1.7 mmol) in CH_2Cl_2 (40 ml) for 19 h. The reaction mixture was then filtered through celite and volatiles were removed under reduced pressure. The resulting brown solid was washed with Et_2O and dried in *vacuum*. Yield 0.69 g (83%). MS (ES): *m/z* 841, $[Ag(ligand)_2]^+$. ^1H NMR ($CDCl_3$, 400 MHz, 298K): δ 8.34 (d, $^3J_{HH}$ = 7.9 Hz, 1H, H_{py}), 8.11 (d, $^3J_{HH}$ = 1.8 Hz, 1H, H_{imi}), 7.98 (t, $^3J_{HH}$ = 7.9 Hz, $^3J_{HH}$ = 7.9 Hz, 1H, H^4_{py}), 7.32 (d, $^3J_{HH}$ = 7.9 Hz, 1H, H_{py}), 7.26–7.19 (m, 1H, H^4_{Ar}), 7.13 (d, $^3J_{HH}$ = 7.6 Hz, 1H, H^3_{Ar} + H^5_{Ar}), 7.03 (d, $^3J_{HH}$ = 1.8 Hz, 1H, H_{imi}), 6.97 (s, 2H, H_{Mes}), 2.33 (s, 3H, *p*-mesityl Me), 2.12 (s, 6H, *o*-mesityl Me), 2.03 (s, 6H, *o*-Ar Me); $^{13}C\{^1H\}$MR ($CDCl_3$, 100 MHz, 298K): δ 159.8 (C_{py}), 150.6 (C_{py}), 140.0 (C^4_{py}), 139.9, 139.2, 136.0, 135.8, 134.7, 129.8, 128.7, 128.0 (8 × C_{Ar+Mes}), 125.1 (C^5_{py}), 123.1 (C_{im}), 120.7 (C_{im}), 113.6 (C^3_{py}), 21.3 (*p*-mesityl Me), 20.7 (*o*-Ar Me), 18.1 (*o*-mesityl Me); The carbene carbon was not observed. Anal. Calcd. for $C_{25}H_{25}AgBrN_3$ (555.26): C 54.08, H 4.54, N 7.57. Found: C 54.59, H 4.34, N 7.59.

Complex 3a. A solution of **2a** (0.23 g, 0.50 mmol) in CH_2Cl_2 (25 ml) was added dropwise to a solution of $[PdBr_2(cod)]$ (0.19 g, 0.50 mmol) in CH_2Cl_2 (25 ml) and stirred at room temperature for 19 h under exclusion from light. The reaction mixture was then filtered through celite and volatiles were removed under reduced pressure. The resulting yellow solid was washed with Et_2O and dried *in vacuum*. Yield 0.18 g (67%). Recrystallization from $DMSO/Et_2O$ gave an analytically pure sample. MS (ES): *m/z* 382, [Pd (ligand)]$^+$. ^1H NMR (DMSO–d_6, 500 MHz, 363K): δ 9.07 (br s, 1H, H^6_{py}), 8.12 (t, $^3J_{HH}$ = 7.6 Hz, 1H, H^4_{py}), 7.83

(d, $^3J_{HH}$ = 7.6 Hz, 1H, H^3_{py}), 7.75 (d, $^3J_{HH}$ = 1.5 Hz, 1H, H_{imi}), 7.59 (t, $^3J_{HH}$ = 7.6 Hz, 1H, H^5_{py}), 7.28 (d, $^3J_{HH}$ = 1.5 Hz, 1H, H_{imi}), 6.99 (s, 2H, H_{Mes}), 5.80 (br s, 2H, CH_2), 2.32 (s, 3H, *p*-mesityl Me), 2.03 (br s, 6H, *o*-mesityl Me). $^{13}C\{^1H\}$ NMR (DMSO–d_6, 126 MHz, 363K): δ 153.9 (C^6_{py}), 152.8 (C^2_{py}), 139.9 (C^4_{py}), 137.7, 134.9, 134.1, 128.3 (4 × C_{Mes}), 124.6 (C^5_{py}), 124.4 (C_{Im}), 124.1 (C^5_{py}), 122.0 (C_{Im}), 54.2 (CH_2), 20.1 (*p*-mesityl Me), 17.6 (*o*-mesityl Me). The carbene carbon was not observed. Anal. Calcd. for $C_{18}H_{19}Br_2N_3Pd$ (543.59) × DMSO: C 38.64, H 4.05, N 6.76. Found: C 38.22, H 3.89, N 6.52.

Complex 3b. A solution of **2b** (0.24 g, 0.52 mmol) in CH_2Cl_2 (25 ml) was added dropwise to a solution of [$PdBr_2$(cod)] (0.20 g, 0.52 mmol) in CH_2Cl_2 (25 ml) and stirred at room temperature for 15 h under exclusion from light. The reaction mixture was then filtered through celite and volatiles were removed under reduced pressure. The resulting yellow solid product was washed with Et_2O and dried *in vacuum*. Yield 0.26 g (95%). Recrystallization from DMSO/Et_2O gave an analytically pure sample suitable for X-Ray. MS (ES): *m/z* 450, $[PdBr(ligand)]^+$. ^1H NMR (DMSO–d_6, 400 MHz, 298K): δ 9.31 (br s, 1H, H^6_{py}), 8.67 (d, $^3J_{HH}$ = 2.1 Hz, 1H, H_{imi}), 8.47–8.37 (m, 1H, H^4_{py}), 8.27 (d, $^3J_{HH}$ = 8.2 Hz, 1H, H^3_{py}), 7.72–7.64 (m, 1H, H^5_{py}), 7.59 (d, $^3J_{HH}$ = 2.1 Hz, 1H, H_{imi}), 6.97 (s, 2H, H_{Mes}), 2.30 (s, 3H, *p*-mesityl Me), 2.02 (s, 6H, *o*-mesityl Me). $^{13}C\{^1H\}$ NMR (DMSO–d_6, 100 MHz, 298K): δ 151.3 (C^2_{py}), 150.1 (C^6_{py}), 142.8 (C^4_{py}), 138.4, 135.5, 134.1, 128.8 (4 × C_{Mes}), 125.5 (C_{Im}), 123.6 (C^5_{py}), 117.8 (C_{Im}), 112.7 (C^3_{py}), 20.7 (*p*-mesityl Me), 17.6 (*o*-mesityl Me). The carbene carbon was not observed. Anal. Calcd. for $C_{17}H_{17}Br_2N_3Pd$ (529.56): C 38.56, H 3.24, N 7.93. Found: C 38.40, H 3.05, N 7.68.

Complex 4a. $AgPF_6$ (0.12 g, 0.46 mmol) was added in one portion to a solution of **3a** (0.12 g, 0.22 mmol) in MeCN (5 ml) and stirred at room temperature for 13 h under exclusion from light. The reaction mixture was then filtered through celite and the volatiles were removed under reduced pressure. The resulting off white solid was washed with Et_2O and dried *in vacuum*. Yield 0.12 g (70%). Recrystallization from CH_2Cl_2/Et_2O gave an analytically pure sample. MS (ES): *m/z* 383, $[Pd(ligand)]^+$. ^1H NMR (CD_3CN, 400 MHz, 298K): δ 8.70 (d, $^3J_{HH}$ = 5.2 Hz, 1H, H^6_{py}), 8.19 (td, $^3J_{HH}$ = 7.6 Hz, $^4J_{HH}$ = 1.0 Hz, 1H, H^4_{py}), 7.85 (d, $^3J_{HH}$ = 7.6 Hz, 1H, H^3_{py}), 7.66–7.57 (m, 2H, H^5_{py} + H_{imi}), 7.23 (d, $^3J_{HH}$ = 1.9 Hz, 1H, H_{imi}), 7.17 (s, 2H, H_{Mes}), 5.69 (s, CH_2), 2.39 (s, 3H, *p*-mesityl Me), 2.09 (s, 6H, *o*-mesityl Me). $^{13}C\{^1H\}$ NMR (CD_3CN, 100 MHz, 298K): δ 155.0 (C^6_{py}), 154.0 (C^2_{py}), 143.6 (C^4_{py}), 141.8 (C_{Mes}), 140.0

($C_{carbene}$), 136.2, 134.4, 130.5 (3 × C_{Mes}), 128.0 (C^3_{py}), 127.4 (C^5_{py}), 126.0 (C_{Im}), 125.0 (C_{Im}), 21.1 (*p*-mesityl Me), 18.2 (*o*-mesityl CH_3). Anal. Calcd. for $C_{22}H_{25}F_{12}N_5P_2Pd$ (755.82) × 1/4 CH_2Cl_2: C 34.39, H 3.31, N 9.01. Found: C 34.40, H 3.18, N 8.82.

Complex 4b. $AgPF_6$ (0.15 g, 0.57 mmol) was added to a solution of **3b** (0.15 g, 0.27 mmol) in MeCN (5 ml) and stirred at room temperature for 16 h under exclusion from light. The reaction mixture was then filtered through celite and the volatiles were removed under reduced pressure. The resulting off white solid was washed with Et_2O and dried *in vacuum*. Yield 0.15 g (88%). Recrystallization from CH_2Cl_2/Et_2O gave an analytically pure sample. MS (ES): *m/z* 369, $[Pd(ligand)]^+$. ^1H NMR (CD_3CN, 400 MHz, 298K): δ 8.53 (d, $^3J_{HH}$ = 5.2 Hz, 1H, H^6_{py}), 8.49–8.39 (m, 1H, H^4_{py}), 8.16 (d, $^3J_{HH}$ = 2.1 Hz, 1H, H_{imi}), 7.99 (d, $^3J_{HH}$ = 8.3 Hz, 1H, H^3_{py}), 7.68–7.58 (m, 1H, H^5_{py}), 7.36 (d, $^3J_{HH}$ = 2.1 Hz, 1H, H_{imi}), 7.16 (s, 2H, H_{Mes}), 2.35 (s, 3H, *p*-mesityl Me), 2.14 (s, 6H, *o*-mesityl Me). $^{13}C\{^1H\}$ NMR (CD_3CN, 100 MHz, 298K): δ 152.6 (C^2_{py}), 152.0 (C^6_{py}), 148.0 ($C_{carbene}$), 146.6 (C^4_{py}), 141.1, 138.8, 138.8, 130.6 (4 × C_{Mes}), 126.3 (C_{Im}), 125.7 (C^5_{py}), 119.9 (C_{Im}), 114.8 (C^3_{py}), 21.2 (*p*-mesityl Me), 17.8 (*o*-mesityl Me). Anal. Calcd. for $C_{21}H_{23}F_{12}N_5P_2Pd$ (741.79) × 1/2 CH_2Cl_2: C 32.93, H 3.08, N 8.93. Found: C 33.35, H 2.94, N 9.04.

Complex 4c. A solution of **2c** (0.08 g, 0.1 mmol) in MeCN (8 ml) was added dropwise to a solution of $[PdBr_2(cod)]$ (0.05 g, 0.1 mmol) in MeCN (8 ml) and stirred at room temperature for 14 h under exclusion from light. The reaction mixture was then filtered through celite and solvent was removed under reduced pressure. The resulting solid was dissolved in CH_2Cl_2, filtered through celite and volatiles were removed under reduced pressure. The residue, supposedly **3c** (see Results and Discussion section), was used in the next step without further purification. $AgPF_6$ (0.08 g, 0.3 mmol) was added to a solution of this residue in MeCN (10 ml) and stirred at room temperature for 21 h under exclusion from light. The reaction mixture was then filtered through celite and volatiles were removed under reduced pressure. The resulting off white solid was dissolved in CH_2Cl_2 (10 ml) and the solution was stirred with activated charcoal for 30 min. The mixture was then filtered through celite and concentrated to 3 ml. An off white solid was precipitated by addition of excess Et_2O, filtered and dried *in vacuum*. Yield 0.065 g (65% from **2c**). MS (ES): *m/z* 473, $[Pd(ligand)+H]^+$. ^1H NMR (CD_3CN, 400 MHz, 298K): δ 8.45 (d, $^3J_{HH}$ = 8.0 Hz 1H, H^4_{py}), 8.21 (d, $^3J_{HH}$ = 2.3 Hz, 1H, H_{imi}), 8.00 (dd, $^3J_{HH}$ = 8.0 Hz, $^4J_{HH}$ = 1.0 Hz, 1H, H_{py}), 7.46 (dd, $^3J_{HH}$ = 8.0 Hz, $^4J_{HH}$ = 1.1 Hz

1H, H_{py}), 7.39–7.33 (m, 3H, H^3_{Ar} + H^5_{Ar} + H_{imi}), 7.23 (d, $^3J_{HH}$ = 7.8 Hz, 1H, H^4_{Ar}), 7.15 (s, 2H, H_{Mes}), 2.33 (s, 3H, *p*-mesityl Me), 2.19 (s, 6H, *o*-mesityl Me), 2.15 (s, 6H, *o*-Ar Me); $^{13}C\{^1H\}$ NMR ($CDCl_3$, 100 MHz, 298K): δ 163.2 (C_{py}), 153.6 (C_{py}), 146.5 (C^4_{py}), 145.4 ($C_{carbene}$), 142.6, 138.7, 138.0, 136.4, 134.1, 132.4, 130.6, 128.9, (8 × C_{Ar} + C_{Mes}), 128.2 (C_{py}), 126.8 (C_{im}), 120.0 (C_{im}), 113.5 (C_{py}), 21.2 (*p*-mesityl Me), 20.7 (*o*-Ar Me), 17.9 (*o*-mesityl Me). Anal. Calcd. for $C_{29}H_{31}F_{12}N_5P_2Pd$ (845.94): C 41.17, H 3.69, N 8.28. Found: C 41.53, H 3.78, N 7.99.

Complex 5b. A solution of **2b** (0.59 g, 1.3 mmol) in CH_2Cl_2 (40 ml) was added dropwise to a solution of [PdBr(Me)(cod)] (0.40 g, 1.3 mmol) in CH_2Cl_2 (40 ml) and stirred at room temperature for 15 h under exclusion from light. The reaction mixture was then filtered through celite and volatiles were removed under reduced pressure. The resulting light brown solid was washed with Et_2O and dried *in vacuum*. Yield 0.58 g (95%). MS (ES): *m/z* 384, $[PdMe(ligand)]^+$. ^1H NMR (DMSO–d_6, 400 MHz, 298K): δ 9.04 (d, $^3J_{HH}$ = 4.6 Hz, 1H, H^6_{py}), 8.58 (d, $^3J_{HH}$ = 2.1 Hz, 1H, H_{imi}), 8.28 (td, $^3J_{HH}$ = 7.8 Hz, $^4J_{HH}$ = 1.6 Hz, 1H, H^4_{py}), 8.17 (d, $^3J_{HH}$ = 7.8 Hz, 1H, H^3_{py}), 7.65–7.69 (m, 1H, H^5_{py}), 7.56 (d, $^3J_{HH}$ = 2.1 Hz, 1H, H_{imi}), 7.06 (s, 2H, H_{Mes}), 2.32 (s, 3H, *p*-mesityl Me), 2.05 (s, 6H, *o*-mesityl Me), 0.01 (s, 3H, Pd–Me). $^{13}C\{^1H\}$ NMR (DMSO–d_6, 100 MHz, 298K): δ 170.2 ($C_{carbene}$), 150.3 (C^2_{py}), 148.7 (C^6_{py}), 141.4 (C^4_{py}), 139.7, 134.8, 134.2, 128.7 (4 × C_{Mes}), 125.2 (C_{Im}), 123.5 (C^5_{py}), 117.4 (C_{Im}), 111.6 (C^3_{py}), 20.7 (*p*-mesityl Me), 17.2 (*o*-mesityl Me), –14.0 (Pd–Me). Anal. Calcd. for $C_{18}H_{20}BrN_3Pd$ (464.70) × 1/4 CH_2Cl_2: C 45.11, H 4.25, N 8.65. Found: C 44.77, H 4.18, N 8.39.

Complex 6a. $AgPF_6$ (0.08 g, 0.3 mmol) was added to a solution of **5a** (0.15g, 0.31 mmol) in MeCN (5 ml) and stirred at room temperature for 16 h under exclusion from light. The reaction mixture was then filtered through celite and volatiles were removed under reduced pressure. The resulting off white solid was dissolved in CH_2Cl_2 (5 ml) and the solution was stirred with activated charcoal for 30 min. The mixture was then filtered through celite and concentrated to 2 ml. An off white solid was precipitated by addition of excess Et_2O, filtered and dried *in vacuum*. Yield 0.13g (72%). X-Ray quality crystals were obtained by layering CH_2Cl_2 solution with Et_2O. MS (ES): *m/z* 398, $[PdMe(ligand)]^+$. ^1H NMR (CD_3CN, 400 MHz, 298K): δ 8.64 (dd, $^3J_{HH}$ = 5.3 Hz, $^4J_{HH}$ = 1.4 Hz, 1H, H^6_{py}), 8.01 (td, $^3J_{HH}$ = 7.7 Hz, $^4J_{HH}$ = 1.4 Hz, 1H, H^4_{py}), 7.71 (d, $^3J_{HH}$ = 7.7 Hz, 1H, H^3_{py}), 7.52 (ddd, $^3J_{HH}$ = 7.7 Hz, $^3J_{HH}$ = 5.3 Hz, $^4J_{HH}$ = 1.2 Hz, 1H, H^5_{py}), 7.45 (d, $^3J_{HH}$ = 2.0 Hz, 1H, H_{imi}), 7.03 (m, 3H, H_{imi} + H_{Mes}), 5.48 (s, 2H,

CH_2), 2.34 (s, 3H, *p*-mesityl Me), 2.02 (s, 6H, *o*-mesityl Me), –0.10 (s, 3H, Pd–Me). $^{13}C\{^1H\}$ NMR (CD_3CN, 100 MHz, 298K): δ 168.0 ($C_{carbene}$), 153.8 (C^2_{py}), 152.4 (C^6_{py}), 140.9 (C^4_{py}), 140.4, 136.4, 136.1, 129.9 (4 × C_{Mes}), 126.3 (C^5_{py}), 126.0 (C^3_{py}),124.3 (C_{Im}), 123.3 (C_{Im}), 56.1 (CH_2), 21.2 (*p*-mesityl Me), 18.4 (*o*-mesityl Me), –13.0 (Pd–Me). Anal. Calcd. for $C_{21}H_{25}F_6N_4PPd$ (584.83) × 1/4 CH_2Cl_2: C 42.11, H 4.24, N 9.24. Found: C 42.38, H 4.40, N 9.32.

Complex 6b. $AgPF_6$ (0.29 g, 1.1 mmol) was added to a solution of **5b** (0.50 g, 1.1 mmol) in MeCN (15 ml) and stirred at room temperature for 18 h under exclusion from light. The reaction mixture was then filtered through celite and volatiles were removed under reduced pressure. The resulting off white solid was dissolved in CH_2Cl_2 (15 ml) and the solution was stirred with activated charcoal for 30 min. The mixture was then filtered through celite and concentrated to 5 ml. An off white solid was precipitated by addition of excess Et_2O, filtered and dried *in vacuum*. Yield 0.56 g (91%). X-Ray quality crystals were obtained by layering CH_2Cl_2 solution with Et_2O. MS (ES): *m/z* 384, $[PdMe(ligand)]^+$. ^1H NMR (CD_3CN, 400 MHz, 298K): δ 8.51 (dd, $^3J_{HH}$ = 5.3 Hz, $^4J_{HH}$ = 1.3 Hz, 1H, H^6_{py}), 8.24 (ddd, $^3J_{HH}$ = 8.3 Hz, $^3J_{HH}$ = 7.7 Hz, $^4J_{HH}$ = 1.3 Hz, 1H, H^4_{py}), 8.05 (d, $^3J_{HH}$ = 2.3 Hz, 1H, H_{imi}), 7.85 (d, $^3J_{HH}$ = 7.7 Hz, 1H, H^3_{py}), 7.58 (ddd, $^3J_{HH}$ = 7.7 Hz, $^3J_{HH}$ = 5.3 Hz, $^4J_{HH}$ = 0.9 Hz, 1H, H^5_{py}), 7.19 (d, $^3J_{HH}$ = 2.3 Hz, 1H, H_{imi}), 7.07 (s, 2H, H_{Mes}), 2.34 (s, 3H, *p*-mesityl Me), 2.06 (s, 6H, *o*-mesityl Me), 0.01 (s, 3H, Pd–Me). $^{13}C\{^1H\}$ NMR (CD_3CN, 100 MHz, 298K): δ 168.5 ($C_{carbene}$), 151.3 (C^2_{py}), 149.1 (C^6_{py}), 143.3 (C^4_{py}), 141.1, 138.8, 138.8, 130.1 (4 × C_{Mes}), 126.5 (C_{Im}), 125.2 (C^5_{py}), 118.8 (C_{Im}), 113.1 (C^3_{py}), 21.2 (*p*-mesityl Me), 17.8 (*o*-mesityl Me), –10.9 (Pd–Me).). Anal. Calcd. for $C_{20}H_{23}F_6N_4PPd$ (570.81) × 1/2 Et_2O: C 43.47, H 4.64, N 9.22. Found: C 43.48, H 4.49, N 9.06.

Complex 6c. A solution of **2c** (0.61 g, 1.1 mmol) in MeCN (5 ml) was added dropwise to a solution of [PdCl(Me)(cod)] (0.29 g, 1.1 mmol) in MeCN (70 ml) and stirred at room temperature for 21 h under exclusion from light. The reaction mixture was then filtered through celite and all volatiles were removed under reduced pressure. The resulting grey solid was dissolved in CH_2Cl_2, again filtered through celite and the solvent was removed under reduced pressure. The residue was used in the next step without further purification. $AgPF_6$ (0.31 g, 1.2 mmol) was added to a solution of this residue in MeCN (75 ml) and stirred at room temperature for 16 h under exclusion from light. The reaction mixture was then filtered

through celite and volatiles were removed under reduced pressure. The resulting off white solid was dissolved in CH_2Cl_2 (30 ml) and the solution was stirred with activated charcoal for 30 min. Mixture was then filtered through celite and concentrated to 10 ml. An off white solid was precipitated by addition of excess Et_2O, filtered and dried *in vacuum*. Yield 0.58 g (78% from **2c**). X-Ray quality crystals were obtained by layering CH_2Cl_2 solution with Et_2O. MS (ES): *m/z* 473, $[Pd(ligand)+H]^+$. ^1H NMR (CD_3CN, 400 MHz, 298K): δ 8.26 (dd, $^3J_{HH}$ = 8.2 Hz, $^3J_{HH}$ = 7.7 Hz 1H, H^4_{py}), 8.10 (d, $^3J_{HH}$ = 2.3 Hz, 1H, H_{imi}), 7.85 (dd, $^3J_{HH}$ = 8.2 Hz, $^4J_{HH}$ = 1.0 Hz, 1H, H_{py}), 7.38 (dd, $^3J_{HH}$ = 7.7 Hz, $^4J_{HH}$ = 1.0 Hz 1H, H_{py}), 7.28 (dd, $^3J_{HH}$ = 8.2 Hz, $^3J_{HH}$ = 7.7 Hz, 1H, H^4_{Ar}), 7.22–7.16 (m, 3H, H^3_{Ar} + H^5_{Ar} + H_{imi}), 7.03 (s, 2H, H_{Mes}), 2.33 (s, 3H, *p*-mesityl Me), 2.13 (s, 6H, *o*-mesityl Me), 2.03 (s, 6H, *o*-Ar Me), 0.00 (s, 3H, Pd–Me).; $^{13}C\{^1H\}$ NMR ($CDCl_3$, 100 MHz, 298K): δ 168.1 ($C_{carbene}$), 160.8 (C_{py}), 151.8 (C_{py}), 143.3 (C^4_{py}), 141.1, 139.5, 137.5, 135.9, 135.7, 131.0, 130.1, 128.6 (8 × C_{Ar} + C_{Mes}), 126.9 (C^5_{py}), 126.9 (C_{im}), 119.0 (C_{im}), 111.7 (C^3_{py}), 21.2 (*p*-mesityl Me), 20.7 (*o*-Ar Me), 17.8 (*o*-mesityl Me), –8.5 (Pd–Me). Anal. Calcd. for $C_{28}H_{31}F_6N_4PPd$ (674.12): C 49.83, H 4.63, N 8.30. Found: C 49.54, H 4.36, N 8.18.

High pressure polymerization reactions. All high pressure polymerization experiments were carried out in a Büchi "tinyclave steel" reactor equipped with an interchangeable 25 mL glass vessel. The reactor was loaded with reactants and pressurized with ethylene. Reaction mixtures were stirred for 24 h at a constant temperature. At the end of each experiment the reactor was vented, cooled to room temperature and a sample was withdrawn for GS-MS and GC analyses. Solutions were filtered over Celite to remove palladium black and solvents were removed under reduced pressure. The residual oils were analyzed by NMR spectroscopy.

Styrene dimerization reactions. Styrene dimerization experiments were carried out in a thermostated three-necked 75 mL glass reactor equipped with a magnetic stirrer and charged with the precatalyst and the solvent. After reaching the reaction temperature, styrene was added and the mixture was stirred for 24 h. Samples for GC analysis were withdrawn at 2 h intervals for the first 8 h and finally at 24 h. Upon cooling the reaction mixture to room temperature two layers were formed and the top layer was collected. Any residual styrene and the solvent were removed under reduced pressure. The residue was dried under vacuum and analyzed by NMR spectroscopy.

Crystal structure determination. Crystal data for **3b**, **4a** and **6a** were collected using a Bruker SMART APEX CCD area detector diffractometer. A full sphere of reciprocal space was scanned by phi-omega scans. Pseudo-empirical absorption correction based on redundant reflections was performed by the program SADABS.[38] Crystal data for **5b**, **6b** and **6c** were collected using an Oxford Diffraction SuperNova A diffractometer fitted with an Atlas detector. At least a complete dataset was collected, assuming that the Friedel pairs are not equivalent. Diffraction data for **7** were collected on a Nonius DIP-1030H system. A total of 30 frames were collected, each with an exposure time of 20 min, rotation angle of 6° about φ. All diffractometers were equipped with Mo–Kα radiation (0.71073 Å). An analytical absorption correction based on the shape of the crystal was performed for all these crystals.[39] The structures were solved by direct methods using SHELXS-97[40] and refined by full matrix least-squares on F^2 for all data using SHELXL-97. Their isotropic thermal displacement parameters were fixed to 1.2 times (1.5 times for methyl groups) the equivalent one of the parent atom. Anisotropic thermal displacement parameters were used for all non-hydrogen atoms. One of the two crystallographically independent complexes of 7 comprises a methyl ligand that is partially substituted by a chloride (refined occupancies of 0.68(1)/0.32(1)). Crystal data and details of refinements are compiled in the supporting information (Table S1). CCDC numbers 844760–844765 and 849648 contain the supplementary crystallographic data for this paper. These data can be obtained free of charge from the Cambridge Crystallographic Data Centre via www.ccdc.cam.ac.uk/data_request/cif.

Acknowledgements. We thank Yannick Ortin for NMR spectroscopic measurements and the Swiss National Science Foundation, University College Dublin, and the Italian MIUR (PRIN N° 207HMTJWP_002) for financial support. Fondazione CRTrieste is gratefully acknowledged for the generous donation of a Varian 500 MHz spectrometer to the Dipartimento di Scienze Chimiche e Farmaceutiche, and the Fondazione Benefica "Kathleen Foreman Casali" for the generous donation of the Büchi tinyclave glass reactor. We thank COST Action D40 for enabling two STSMs of V.K. to Trieste.

Supporting Information Available: NMR plots, crystallographic details, and crystallographic data in CIF format. This material is available free of charge via the internet at http://pubs.acs.org.

References

(1) (a) Ittel, S. D.; Johnson, L. K.; Brookhart, M. *Chem. Rev.* **2000**, *100*, 1169. (b) Alt, H. G.; Köppl, A. *Chem. Rev.* **2000**, *100*, 1205. (c) Coates, G. W. *Chem. Rev*. **2000**, *100*, 1223. (d) Resconi, L.; Cavallo, L.; Fait, A.; Piemontesi, F. *Chem. Rev*. **2000**, *100*, 1253. (e) Chen, E. Y.-X.; Marks, T. *Chem. Rev.* **2000**, *100*, 1391. (f) Gibson, V. C.; Spitzmesser, S. K. *Chem. Rev*. **2003**, *103*, 283. (g) Claver, C.; Milani, B. *Dalton Trans.* **2009**, 8783 (themed issue).

(2) (a) Boffa, L. S.; Novak, B. M. *Chem. Rev.* **2000**, *100*, 1479. (b) Sen, A.; Borkar, S., *J. Organomet. Chem.* **2007**, *692*, 3291. (c) Nakamura, A.; Ito, S.; Nozaki, K., *Chem. Rev.* **2009**, *109*, 5215. (d) Berkefeld, A.; Mecking, S. *Angew. Chem. Int. Ed.* **2008**, *47*, 2538. (e) Dong, J.-Y.; Hu, Y. *Coord. Chem. Rev.* **2006,** *250*, 47.

(3) Johnson, L. K.; Killian, C. M.; Brookhart, M. *J. Am. Chem. Soc.* **1995,** *117*, 6414.

(4) For reviews, see: (a) Britovsek, G. J. P.; Gibson, V. C.; Wass, D. F. *Angew. Chem. Int. Ed.* **1999**, *38*, 428. (b) Ittel, S. D.; Johnson, L. K.; Brookhart, M. *Chem. Rev.* **2000**, *100*, 1169. (c) Mecking, S. *Angew Chem. Int. Ed.* **2001**, *40*, 534. (d) Guan, Z. *Chem. Eur. J.* **2002**, *8*, 3086.

(5) For selected examples, see: (a) Guan, Z.; Cotts, P. M.; McCord, E. F.; McLain, S. J. *Science* **1999**, *283*, 2059. (b) Younkin, T. R.; Connor, E. F.; Henderson, J. I.; Friedrich, S. K.; Grubbs, R. H.; Bansleben, D. A. *Science* **2000**, *287*, 460. (c) Schmid, M.; Eberhardt, R.; Klinga, M.; Leskelä, M.; Rieger, B. *Organometallics* **2001,** *20*, 2321. (d) Guan, Z.; Marshall, W. J. *Organometallics* **2002,** *21*, 3580. (e) Wu, F.; Foley, S. R.; Burns, C. T.; Jordan, R. F. *J. Am. Chem. Soc*. **2005**, *127*, 1841. (f) Williams, B. S.; Leatherman, M. D.; White, P. S.; Brookhart, M. *J. Am. Chem. Soc.* **2005**, *127*, 5132.

(6) (a) Johnson, L. K.; Mecking, S.; Brookhart, M. *J. Am. Chem. Soc.* **1996,** *118*, 267. (b) Mecking, S.; Johnson, L. K.; Wang, L.; Brookhart, M. *J. Am. Chem. Soc.* **1998**, *120*, 888.

(7) Popeney, C. S.; Camacho, D. H.; Guan, Z. J. *Am. Chem. Soc.* **2007**, *129*, 10062.

(8) Drent, E.; van Dijk, R.; van Ginkel, R.; van Oort, B.; Pugh, R. I. *Chem. Commun.* **2002**, 744.

(9) Guironnet, D.; Roesle, P.; Rünzi, T.; Göttker-Schnetmann, I.; Mecking, S. *J. Am. Chem. Soc.* **2009**, *131*, 422.

(10) (a) Vela, J.; Lief, G. R.; Shen, Z.; Jordan, R. F. *Organometallics* **2007,** *26*, 6624. (b) Luo, S.; Vela, J.; Lief, G. R.; Jordan, R. F. *J. Am. Chem. Soc.* **2007,** *129*, 8946. (c) Kochi, T.; Noda, S.; Yoshimura, K.; Nozaki, K. *J. Am. Chem. Soc.* **2007,** *129*, 8948. (d) Weng, W.; Shen, Z.; Jordan, R. F. *J. Am. Chem. Soc.* **2007**, *129*, 15450. (e) Ito, S.; Munakata, K.; Nakamura, A.; Nozaki, K. *J. Am. Chem. Soc.* **2009,** *131*, 14606.

(11) (a) Stockland, R. A.; Jordan, R. F. *J. Am. Chem. Soc.* **2000,** *122*, 6315. (b) Stockland, R. A.; Foley, S. R.; Jordan, R. F. *J. Am. Chem. Soc.* **2002,** *125*, 796. (c) Foley, S. R.; Stockland, R. A.; Shen, H.; Jordan, R. F. *J. Am. Chem. Soc*. **2003**, *125*, 4350. (d) Chen, C.; Luo, S.; Jordan, R. F. *J. Am. Chem. Soc.* **2010,** *132*, 5273. (e) Kilyanek, S. M.; Stoebenau, E. J.; Vinayavekhin, N.; Jordan, R. F. *Organometallics* **2010,** *29*, 1750.

(12) (a) Bourissou, D.; Guerret, O.; Gabbai, F.; Bertrand, G. *Chem. Rev.* **2000**, *100*, 39. (b) Hahn, F. E.; Jahnke, M. C. *Angew. Chem. Int. Ed.* **2008**, *47*, 3122. (c) Arduengo, A. J.; Bertrand, G. *Chem. Rev.* **2009**, *109*, 3209 (thematic issue). (d) Melami, M.; Soleilhavoup, M.; Bertrand, G. *Angew. Chem. Int. Ed*. **2010**, *49*, 8810. (e) Mercs, L.; Albrecht, M. *Chem. Soc. Rev.* **2010**, *39*, 1903.

(13) For a related ligand system comprising a NHC functionalized with an acyclic imine donor-group, see: (a) Al Thagfi, J.; Dastgir, S.; Lough, A. J.; Lavoie, G. G. *Organometallics* **2010**, *29*, 3133. (b) Badaj, A. C.; Dastgir, S.; Lough, A. J.; Lavoie, G. G. *Dalton Trans.* **2010**, *39*, 3361.

(14) During the preparation of this manuscript, a paper appeared on palladium complexes with a chelating N-heterocyclic carbene – sulfonate ligand. The work was based on an analogous approach*, i.e.* aiming at enhancing the electronic asymmetry and at decreasing the metal electrophilicity by replacing the phosphine in Drent's *P,O*-bidentate ligand with a NHC unit: (a) Zhou, X.; Jordan, R. F. *Organometallics* **2011**, *30*, 4632. The synthesis of a related sulfonate-substituted NHC palladium complex was reported recently: (b) Nagai, Y.; Kochi, T.; Nozaki, K. *Organometallics* **2009**, *28*, 6131. For a related C_{NHC},*O*-bidentate system, see also (c) Waltman, A. W.; Grubbs, R. H. *Organometallics* **2004**, *23*, 3105.

(15) (a) Gründemann, S.; Albrecht, M.; Kovacevic, A.; Faller, J. W.; Crabtree, R. H. *J. Chem. Soc., Dalton Trans.* **2002**, 2163. (b) for a recent application of these ligands in selective alkyne transfer semihydrogenation, see: Warkins, S.; Bosman, S.; Weigand, J. J.; Elsevier, C. J. *Appl. Organometal. Chem.* **2011**, *25,* 276.

(16) (a) Tulloch, A. A. D.; Danopoulos, A. A.; Winston, S.; Kleinhenz, S.; Eastham, G. *J. Chem. Soc., Dalton Trans.* **2000**, 4499. (b) Tulloch, A. A. D.; Winston, S.; Danopoulos, A. A.; Eastham, G.; Hursthouse, M. B. *Dalton Trans.* **2003**, 699.

(17) See the supporting information for details.

(18) Leung, C. H.; Incarvito, C. D.; Crabtree, R. H. *Organometallics* **2006**, *25*, 6099.

(19) A complex related to **3a** comprising a methyl instead of a mesityl substituent attached to the carbene was shown to polymerize norbornene upon activation with MAO, which is supposed to generate an analogue of **6a** in situ, see: Wang, X.; Liu, S.; Weng, L.-H.; Jin, G.-X. *Organometallics* **2006**, *25*, 3565.

(20) Olefin dimerization and oligomerization is well established. For reviews, see ref 1; for early examples, see: (a) Keim, W.; Hoffmann, B.; Lodewick, R.; Peukert, M.; Schmitt, G.; Fleischhauer, J.; Meier, U. *J. Mol Catal.* **1979**, *6*, 79. (b) Chauvin, Y.; Gilbert, B.; Guibard, I. *J. Chem. Soc., Chem. Commun.* **1990**, 1715. (c) DiRenzo, G. M.; White, P. S.; Brookhart, M. *J. Am. Chem. Soc.* **1996**, *118*, 6225.

(21) (a) Rix, F. C.; Brookhart, M.; White, P. S. *J. Am. Chem. Soc.* **1996**, *118*, 4746. (b) Siegbahn, P. E. M.; Stromberg, S. *Organometallics* **1996**, *15*, 5542. (c) Sveida, S. A.; Johnson, L. K.; Brookhart, M. *J. Am. Chem. Soc.* **1999**, *121*, 10634.

(22) Similar deviation of the oligomerization rate for complex **6b** is impossible because the amount of inserted ethylene cannot be unambiguously determined; the signals of the terminal CH_3 groups of 1-butene and of higher olefins are superimposed in the ^1H NMR spectrum, and the pertinent CH_2 resonances are partially overlapping with the signals of the ligand of unactivated complex **6b**.

(23) The twofold larger production of butene fractions when using **6c** as catalyst precursor may insinuate a twice higher turnover frequency (TOF) than **6b**. However, when considering the productivity per active palladium site, similar TOFs for **6b** and **6c** are apparent: only about 5% of **6b** are activated (*cf* Fig. 5a, no decomposition observed), while approximately 10% of **6c** are converted to a catalytically active species (*cf* Fig. 5b, 30% consumption of **6c**, though yielding some 20% decomposed material).

(24) (a) Cossee, P. *J. Catal.* **1964**, *3*, 80. (b) Arlman, E. J.; Cossee, P. *J. Catal.* **1964**, *3*, 99. See also: (c) Bhalla, G.; Oxgaard, J.; Goddard, W. A., III; Periana, R. A. *Organometallics* **2005**, *24*, 5499.

(25) (a) Bre, A.; Chauvin, Y.; Commereuc, D. *New J. Chem.* **1986**, *10*, 535. (b) Jolly, W. P. *Acc. Chem. Res.* **1996**, *29*, 544. (c) Agapie, T.; Labinger, J. A.; Bercaw, J. E. *J. Am. Chem. Soc.* **2007**, *129*, 14281. (d) McGuinness, D. S. *Organometallics* **2009**, *28*, 244. (e) McGuinness, D. S. *Chem. Rev.* **2011**, *111*, 2321.

(26) No products from a concerted reductive elimination of the alkyl and carbene moieties have been detected, cf. (a) McGuinness, D. S.; Cavell, K. J. *Organometallics* **2000**, *19*, 4918. (b) McGuinness, D. S.; Saendig, N.; Yates, B. F.; Cavell, K. J. *J. Am. Chem. Soc.* **2001**, *123*, 4029.

(27) (a) McGuinness, D. S.; Müller, W.; Wasserscheid, P.; Cavell, K. J.; Skelton, B. W.; White, A. H.; Englert, U. *Organometallics* **2002**, *21*, 175. (b) Cavell, K. J.; McGuinness, D. S. *Coord. Chem. Rev.* **2004**, *248*, 671. (c) Crudden, C. M.; Allen, D. P. *Coord. Chem. Rev*. **2004**, *248*, 2247. (d) Cavell, K. J. *Dalton Trans.* **2008**, 6676. (e) Heckenroth, M.; Khlebnikov, V.; Neels, A.; Schurtenberger, P.; Albrecht, M. *ChemCatChem* **2011**, *3*, 167.

(28) (a) McGuinness. D. *Dalton Trans*. **2009**, 6915. (b) MacKinnon, A. L.; Baird, M. C. *J. Organomet. Chem.* **2003,** *683*, 114. (c) McGuinness, D. S.; Gibson, V. C.; Wass, D. F.; Steed, J. W. *J. Am. Chem. Soc.* **2003,** *125*, 12716. (d) Danopoulos, A. A.; Wright, J. A.; Motherwell, W. B.; Ellwood, S. *Organometallics* **2004**, *23*, 4807. (e) Wang, X.; Liu, S.; Jin, G.-X. *Organometallics* **2004,** *23*, 6002. (f) Ketz, B. E.; Ottenwaelder, X. G.; Waymouth, R. M. *Chem. Commun.* **2005**, 5693. (g) El-Batta, A.; Waltman, A. W.; Grubbs, R. H. *J. Organomet. Chem.* **2011**, *696,* 2477.

(29) Milani, B.; Marson, A.; Scarel, A.; Mestroni, G.; Ernsting, J. M.; Elsevier, C. J. *Organometallics* **2003**, *22*, 1974.

(30) (a) Skupinska, J. *Chem. Rev*. **1991**, *91*, 613. (b) Speiser, F.; Braunstein, P.; Saussine, L. *Acc. Chem. Res.* **2005**, *38*, 784.

(31) (a) Drent, E.; Budzelaar, P. H. M. *Chem. Rev.* **1996**, *96*, 663. (b) Scarel, A.; Durand, J.; Franchi, D.; Zangrando, E.; Mestroni, G.; Carfagna, C.; Mosca, L.; Seraglia, R.; Consiglio, G.; Milani, B. *Chem. Eur. J.* **2005**, *11*, 6014. (c) Durand, J.; Scarel, A.; Milani, B.; Seraglia, R.; Gladiali, S.; Carfagna, C.; Binotti, B. *Helv. Chim. Acta* **2006**, *89*, 1752.

(32) (a) Scarel, A.; Durand, J.; Franchi, D.; Zangrando, E.; Mestroni, G.; Milani, B.; Gladiali, S.; Carfagna, C.; Binotti, B.; Bronco, S. Gragnoli, T. *J. Organomet. Chem.*

2005, *690*, 2106. (b) Milani, B.; Anzilutti, A.; Vicentini, L.; Sessanta o Santi, A.; Zangrando, E.; Geremia, S.; Mestroni, G. *Organometallics* **1997**, *16*, 5064.

(33) For a related reactivity pattern, see (a) Pillai, S. M.; Ravindranathan, M.; Sivaram, S. *Chem. Rev*. **1986**, *86*, 353. (b) Lee, D. W.; Yi, C. S. *Organometallics* **2010**, *29*, 3413. (c) Fanfoni, L.; Meduri, A.; Zangrando, E.; Castillon, S.; Felluga, F.; Milani, B. *Molecules.* **2011**, *16*, 1804.

(34) (a) Blum, O.; Milstein, D. *J. Am. Chem. Soc.* **1995**, *117*, 4582. (b) Ritter, J. C. M.; Bergman, R. G. *J. Am. Chem. Soc.* **1998**, *120*, 6826. (c) Krug, C.; Hartwig, J. F. *J. Am. Chem. Soc*. **2002**, *124*, 1674.

(35) Scott, Natalie M.; Schareina, T.; Tok, O.; Kempe, R. *Eur. J. Inorg. Chem.*, **2004**, 3297.

(36) Durand, J.; Zangrando, E.; Stener, M.; Fronzoni, G.; Carfagna, C.; Binotti, B.; Kamer, P. C. J.; Müller, C.; Caporali, M.; van Leeuwen, P. W. N. M.; Vogt, D.; Milani, B. *Chem*. *Eur*. *J*., **2006**, *12*, 7639.

(37) (a) Dahan, F.; Dyer, Philip W.; Hanton, Martin J.; Jones, M.; Mingos, D. Michael P.; White, Andrew J. P.; Williams, David J.; Williamson, A.-M. *Eur. J. Inorg. Chem.* **2002**, 732. (b) Rulke, R. E.; Ernsting, J. M.; Spek, A. L.; Elsevier, C. J.; van Leeuwen, P. W. N. M.; Vrieze, K. *Inorg. Chem.* **1993**, *32*, 5769. (c) Evrard, D.; Lucas, D.; Mugnier, Y.; Meunier, P.; Hierso, J. C. *Organometallics* **2008**, *27*, 2643.

(38) Bruker (2001). SADABS, Bruker AXS Inc., Madison, Wisconsin, USA.

(39) Program CrysalisPro Version 1.171.33.55, Oxford Diffraction Limited, 2010. Analytical numeric absorption correction using a multifaceted crystal model were based on expressions derived by Clark and Reid: Clark, R. C.; Reid, J. S. *Acta Cryst.* **1995**, *A51*, 887.

(40) Sheldrick, G. M. *Acta Cryst.* **2008**, *A64*, 112.

Table of Contents entry: